GSA Data Repository 2017354

Evidence for a dynamic grounding-line in outer Filchner Trough, Antarctica, until the early Holocene

Jan Erik Arndt, Claus-Dieter Hillenbrand, Hannes Grobe, Gerhard Kuhn, and Lukas Wacker

MATERIAL, METHODS AND LABORATORY TECHNIQUES

Marine geophysical data

Most of the multibeam bathymetry data and acoustic sub-bottom profiles from the study area (Fig. 1a) were collected on expedition PS96 with RV *Polarstern* in austral summer 2015/2016 using the hull-mounted Atlas-Teledyne Hydrosweep DS3 and Parasound P-70 systems (Schröder, 2016). Pre-existing bathymetric data acquired during expeditions JR97 (2005) with RRS *James Clark Ross* using a Kongsberg-Simrad EM120 system and ANT-VIII/5 (1989/1990) with RV *Polarstern* using an Atlas Hydrosweep DS1 system (Miller and Oerter, 1991) were added to the bathymetry map of the study area. All bathymetric data were corrected on board by applying sound velocity profiles derived from conductivity-temperature-depth casts and post-processed to reject outlying soundings in CARIS Hips & Sips or in MB System, respectively. The final database was jointly gridded at 25 × 25 m resolution with a weighted moving average gridding algorithm in QPS Fledermaus.

Marine geological data

Methods: Gravity cores PS96/079-3 and PS96/080-1 were recovered on cruise PS96 from the study area (Fig. 1a; Table DR1) (Schröder, 2016). Physical properties (magnetic susceptibility, wet bulk density and P-wave velocity) were measured at 1-cm intervals on the whole cores with a GEOTEK multi-sensor core logger (MSCL) at the Alfred Wegener Institute in Bremerhaven. The cores were then split into working and archive halves, and their lithology and sedimentary structures were described visually, using X-radiographs and using smear slides. Shear strength was measured on the working halves of the cores with a hand-held shear vane. Water content and grain-size composition were analyzed on discrete samples taken from the cores. Water content was determined by weighing of the wet and freeze-dried samples, and gravel (>2 mm), sand (63 µm-2 mm) and mud (2 µm-63 µm) contents were analyzed by wet and dry sieving of 1-cm thick sediment samples taken from the working halves of the cores (volume: ca. 50 cm^3). Because gravel content may not be determined in a statistically reliable way on samples of this volume, we only present the sand and mud contents in Figure 2, which inform on the grain-size composition of the matrix of the sediments. Gravel and pebble abundance was evaluated visually and on the X-radiographs. The sand fraction was investigated under a microscope for the presence of calcareous microfossils.

Lithofacies classification and interpretation: The sediments recovered in cores PS96/079-3 and PS96/080-1 were assigned to seven different lithofacies, with each facies occurring in one of the cores only. The characteristics of each lithofacies and

the interpretation of their depositional and their paleoenvironmental settings, which followed previously published literature on lithofacies in marine sediment cores from glaciated continental margins, are given in Table DR1. X-radiograph examples for each lithofacies are given in Figure DR**5**.

Chronology: Two horizons in each core were identified, which contained a few calcareous foraminifer shells (benthic species *Globocassidualina* spp. and *Cibicidoides* spp. and planktic species *Neogloboquadrina pachyderma* sinistral). Importantly, the two dated horizons in core PS96/079-3 are from lithofacies showing no indication of sediment reworking by gravitational downslope or glacial processes (Fig. DR6). All the foraminifer shells were picked for MICADAS AMS ^{14}C dating (Wacker et al., 2010) at the Laboratory of Ion Beam Physics, ETH Zürich. The ^{14}C dates were calibrated with the CALIB 7.1 calibration program (Stuiver and Reimer, 1993) using a regional marine reservoir correction of 1215±30 years (Hillenbrand et al., 2012) and the MARINE13 calibration dataset (Reimer et al., 2013) (Table DR2). For the full set of core photos and X-radiographs of cores PS96/079-3 and PS96/080-1, see https://doi.org/10.1594/PANGAEA.864391 and https://doi.org/10.1594/PANGAEA.864392, respectively.

Table DR1: Summary of lithofacies observed in the studied cores, and inferred processes and paleoenvironments. Preferred interpretations for each lithofacies are underlined. References: 1) McKay et al., 2009; 2) McKay et al., 2012; 3) Passchier et al., 2011; 4) Tripsanas et al., 2008; 5) Hillenbrand et al., 2010; 6) Licht et al., 1999; 7) Domack et al., 1999.

Facies	Core	Depth (cmbsf)	Lithology and sedimentary structure	Depositional process and environmental setting
Ml	PS96/079-3	[156/158]-[162/164]	laminated mud	Hemipelagic suspension settling[1,2]
MGSl	PS96/079-3	0-28 76-117 [129/132]-[156/158] [162/164]-181.5	laminated and stratified mud alternating with gravelly sandy mud and gravelly muddy sand	Suspension settling from turbid plumes[1,3], current-influenced glacimarine deposition[3], hemipelagic sedimentation with deposition of ice-rafted debris (IRD)[1,3]
Mf	PS96/079-3	28-76	folded mud	Debris flow[4], slump[4]
SGMm	PS96/079-3	117-[129/132]	massive gravelly muddy sand with inclined (erosional) base	Redeposition by mass flow[1,3], ice-shelf collapse sediment[3]
MSI	PS96/080-1	25-51	consolidated sandy mud with gravel- to pebble-sized intraclasts	Glacimarine deposition proximal to grounding line[2], mass flow deposit[2]
Dmb	PS96/080-1	0-[10/11]	massive muddy diamicton with some microfossils (here: diatoms)	Glacimarine deposition proximal to grounding line[5,6], iceberg-rafted diamicton[5,7], iceberg turbate[5,6]
Dmt	PS96/080-1	[10/11]-25 51-223	massive, purely terrigenous muddy diamicton	Subglacial till deposition[1-3,5-7], IRD rainout proximal to grounding line[1-3], glacigenic debris flow[1,5]

Table DR2: Locations, conventional and calibrated AMS ^{14}C dates on calcareous microfossils from the investigated and previously published sediment cores from the Weddell Sea (for uncertainties affecting ^{14}C dating of Antarctic shelf sediments, see Heroy and Anderson, 2007). Sample depths are given in centimetres below seafloor (cmbsf). All ^{14}C-dates were corrected using an offset (ΔR) of 815±30 years from the global marine reservoir effect (R) of 400 years in accordance with both an uncorrected ^{14}C-date of seafloor surface sediments from the uppermost continental slope (see conventional ^{14}C-age given in italics) and previous studies from around Antarctica (e.g. RAISED Consortium, 2014). The corrected ^{14}C-dates were calibrated with the CALIB Radiocarbon Calibration Program version 7.1.0html (http://calib.qub.ac.uk/calib/; Stuiver and Reimer, 1993) using the MARINE13 calibration dataset (Reimer et al., 2013). Errors of calibrated dates are given as a 2σ range. The ^{14}C-dates marking minimum ages for grounded ice retreat from a core site are highlighted in bold. Coring devices: GBC: giant box core, GC: gravity core, PH: phleger core, PC: piston core. Dated calcareous microfossils comprise benthic foraminifera (bF: unspecified benthic foraminifera, C: *Cibicides* spp., G: *Globocassidulina* spp.), planktic foraminifera (N: *Neogloboquadrina pachyderma* sinistral) and bryozoans (B). If known, number of dated foraminifer shells is also given. X-radiographs of dated horizons in cores PS96/079-3 and PS96/080-1 are shown in Figure DR6. Preservation of all dated foraminifer shells was modest. References: A) Hillenbrand et al., 2012; B) Stolldorf et al., 2012; C) Anderson and Andrews, 1999.

Area	Cruise	Gear	Core ID	Latitude (°)	Longitude (°)	Water depth (m)	Core recovery (m)	Sample depth (cmbsf)	Laboratory code	Dated microfossils (n)	Conventional ^{14}C age ±error (yrs BP)	R (yrs)	ΔR ±error (yrs)	Calibrated ^{14}C age ±error (cal yrs BP)	Reference
Filchner Trough (outer shelf)	PS96	GC	PS96/79-3	-75.6250	-31.8722	763	1.81	17	ETH-74959.1.1	G (35), C (1)	9995±75	400	815±30	9934±243	this study
								150	ETH-74960.1.1	G (4), C (1), N (3)	**24560±250**	**400**	**815±30**	**27530±387**	this study
Filchner Trough (outer shelf)	PS96	GC	PS96/80-1	-75.6890	-31.7983	720	2.23	20	ETH-74961.1.1	G (28)	14120±90	400	815±30	15436±299	this study
								120	ETH-74962.1.1	G (21)	11415±85	400	815±30	11836±447	this study
E' Crary Fan (uppermost slope)	ANT-IV/3	GBC	PS1418-1	-74.4750	-35.5933	769	4.89	0-1	HD-13273	B	*1215±30*	*N/A*	*N/A*	*[0]*	ref. A
Filchner Trough (mid-shelf)	IWSOE69	PC	G7	-77.3330	-36.5500	1079	1.57	0-5	CCAMS-95867	bF	**9040±100**	400	815±30	**8738±273**	ref. B
Weddell Sea (continental rise)	IWSOE68	PH	37	-69.6833	-46.2670	3777	0.90	56-60	AA-24841	N	26570±490	400	815±30	29580±1092	ref. C
Weddell Sea (continental rise)	IWSOE68	PH	52	-67.3667	-47.3667	3768	0.85	42-47	AA-19910	N (800)	25900±620	400	815±30	28930±1287	ref. C

Figure DR1: Locations of the investigated and previously published sediment cores from the Weddell Sea. Background data from IBCSO V1.0, Arndt et al. 2013.

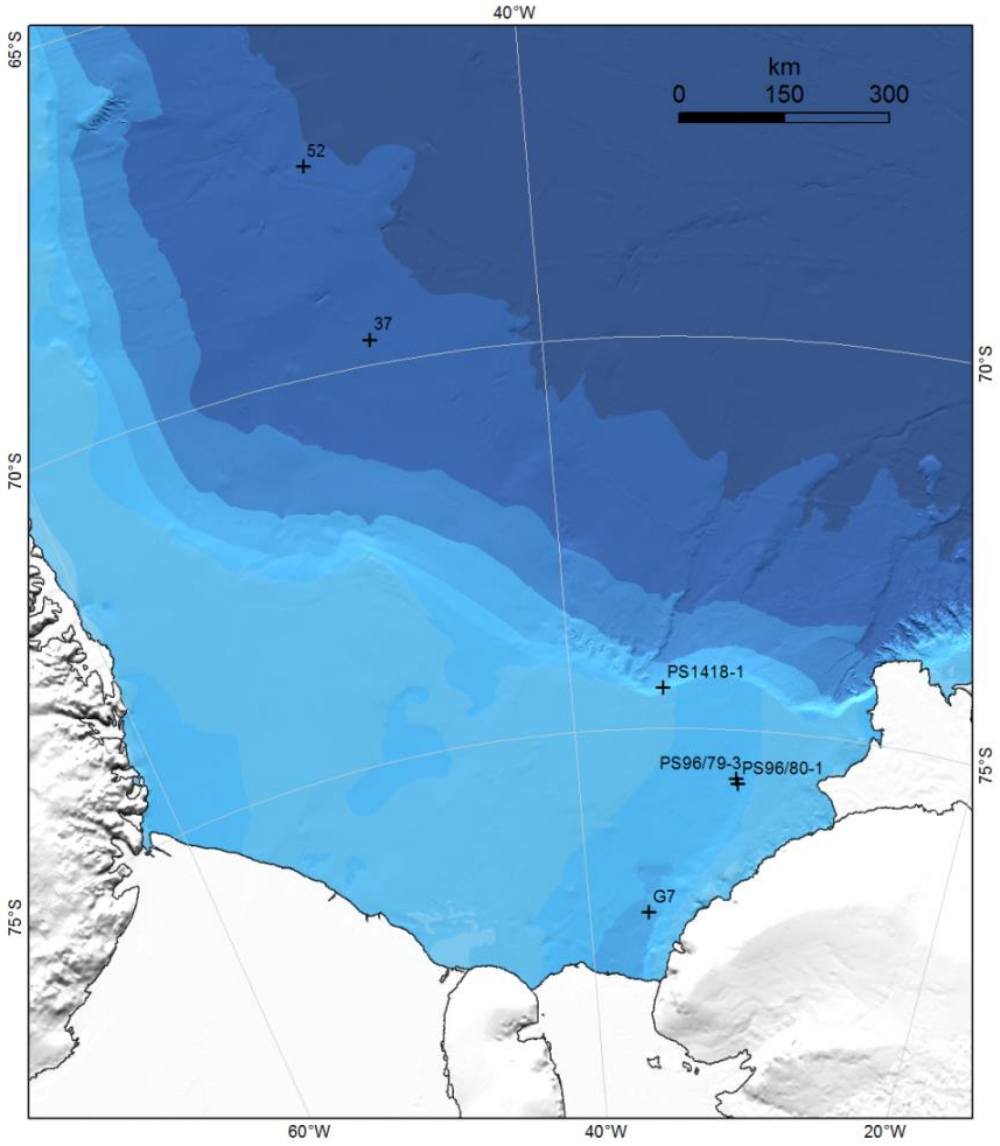

Figure DR2: (A) Line drawing of interpreted submarine landforms with locations of bathymetric profiles: (B) along the trough centre over GZW 1b; (C) across GZW 1a and GZW 1b.

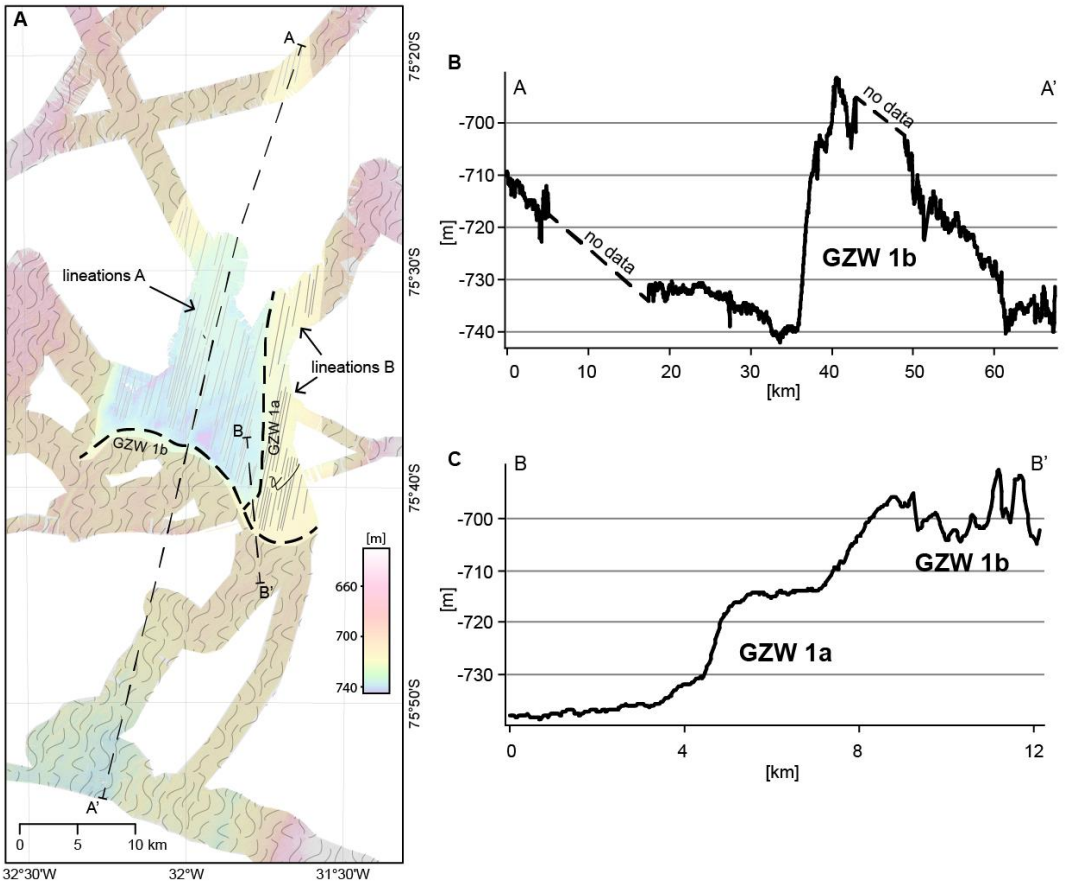

Figure DR3: Detailed sub-bottom profiler (PARASOUND) transects from core locations and other transitions from draped lineations to GZW 1a and 1b.

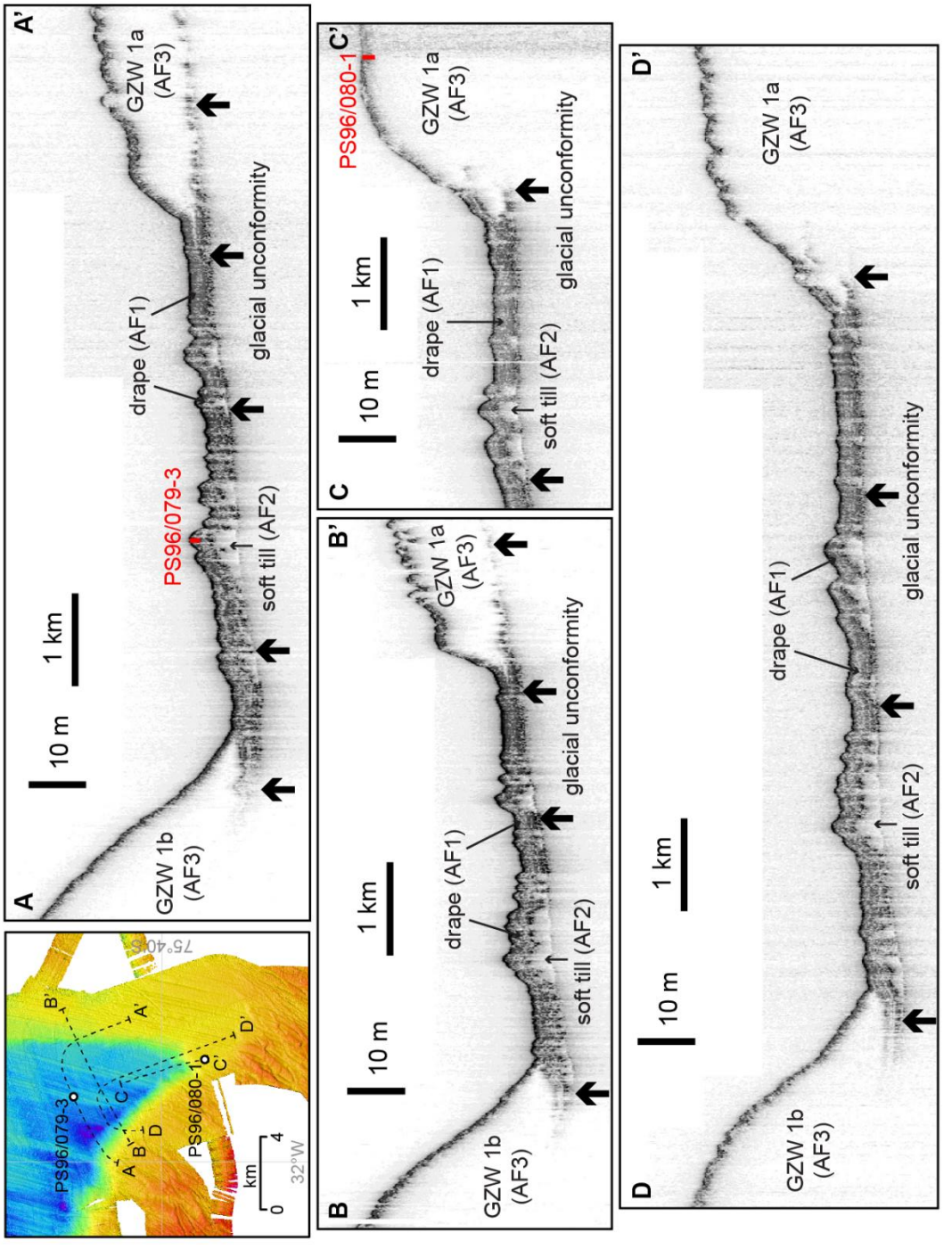

Figure DR4: Detailed bathymetric maps of core locations PS96/079-3 and PS96/080-1.

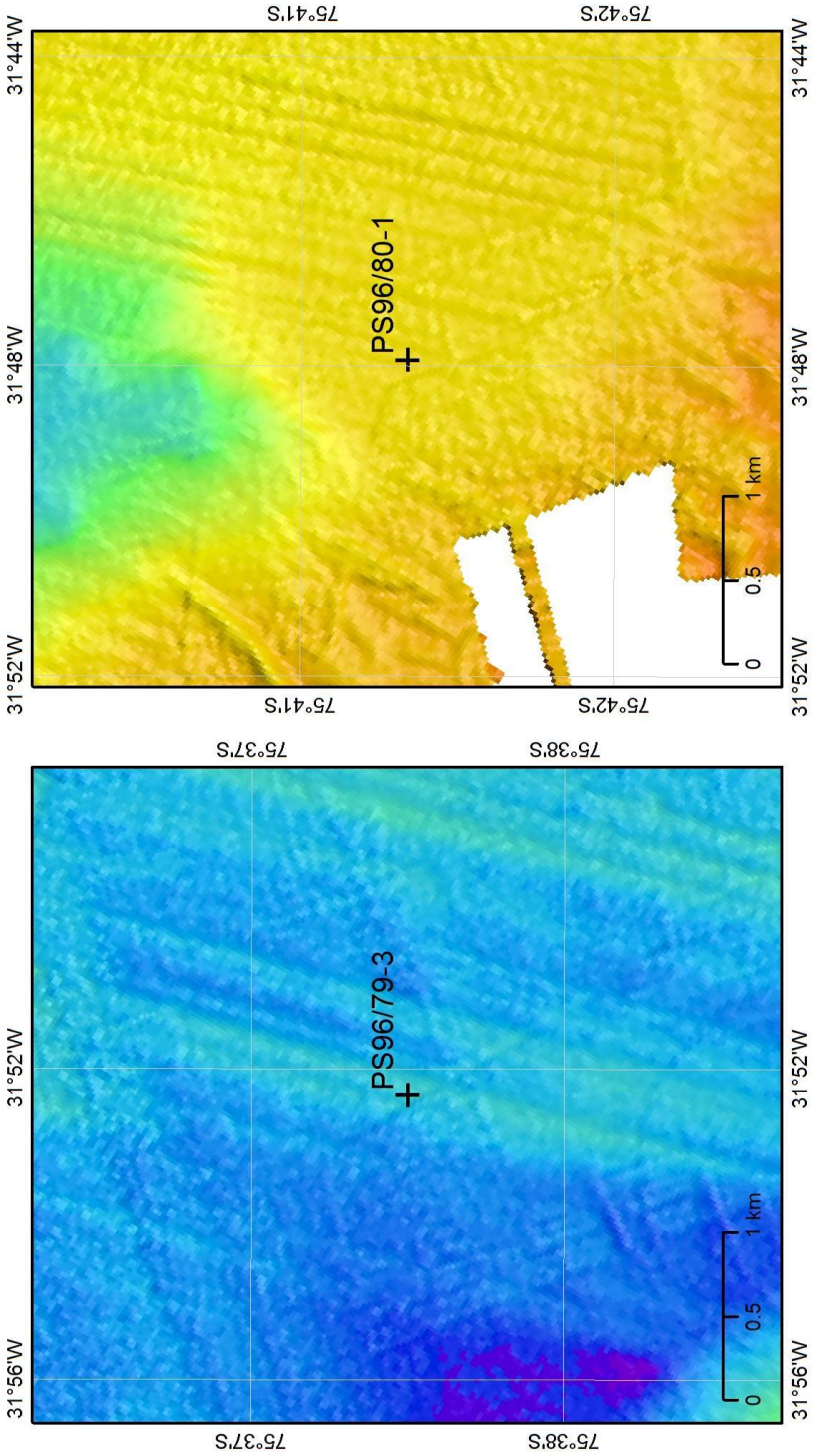

Figure DR5 (next 3 pages): X-radiograph (positives) examples for lithofacies identified in the studied cores. PS96/079-3: a) Laminated mud (Ml) in between laminated and stratified mud alternating with gravelly sandy mud and gravelly muddy sand (MGSl); b) laminated and stratified mud alternating with gravelly sandy mud and gravelly muddy sand (MGSl); c) folded mud (Mf); d) massive gravelly muddy sand with inclined, erosional base (SGMm) on top of laminated and stratified mud alternating with gravelly sandy mud and gravelly muddy sand (MGSl). PS96/080-1: e) consolidated sandy mud with gravel- to pebble-sized intraclasts (MSI); f) massive muddy diamicton with some diatoms (Dmb) on top of massive, purely terrigenous muddy diamicton (Dmt); g) massive, purely terrigenous muddy diamicton (Dmt). Each X-radiograph is 10 cm wide, and white areas are voids in the sediment slabs caused by large gravel grains/pebbles or sample processing.

107 **Figure DR5 (continued)**

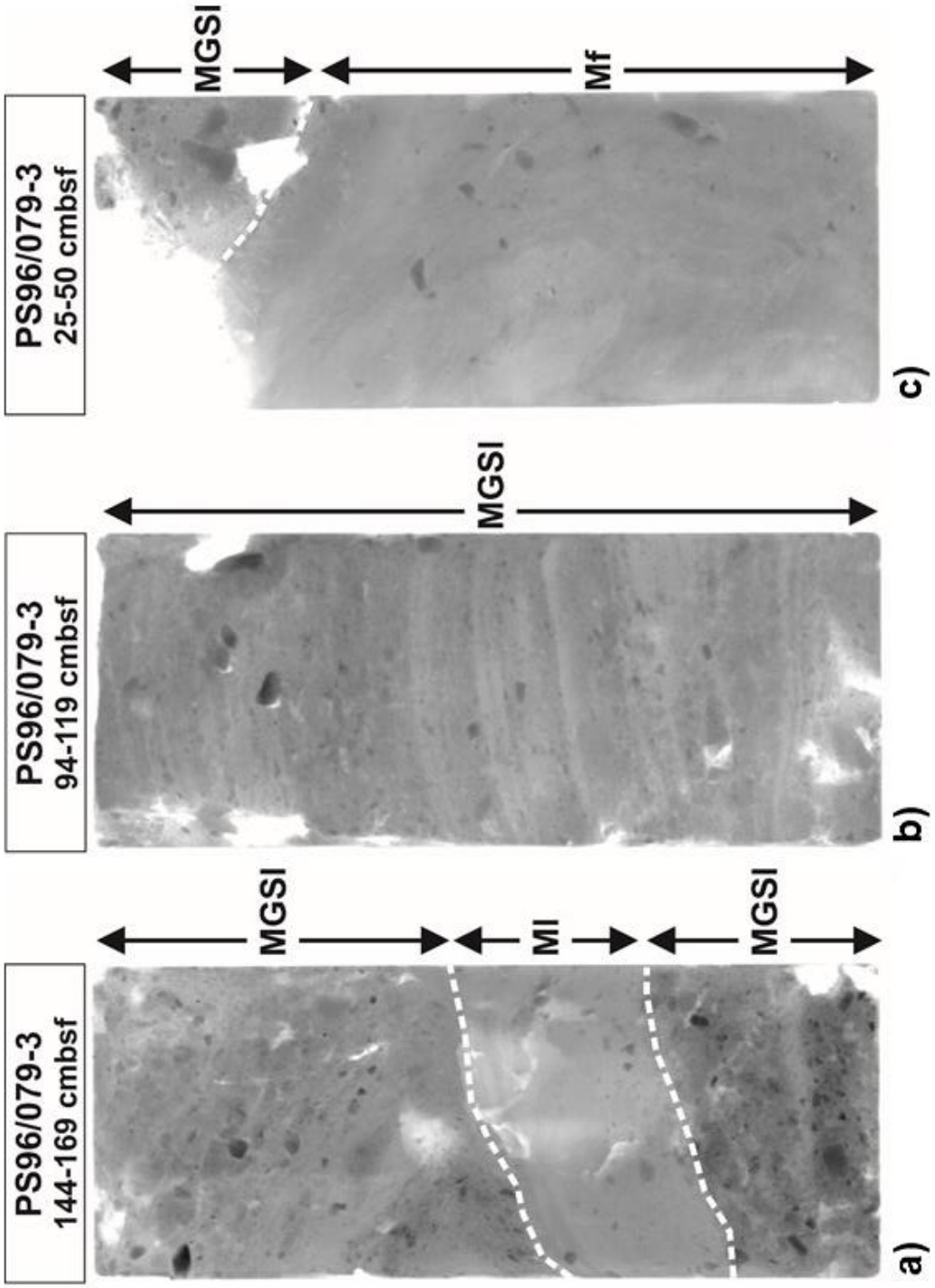

108

109

110 **Figure DR5 (continued)**

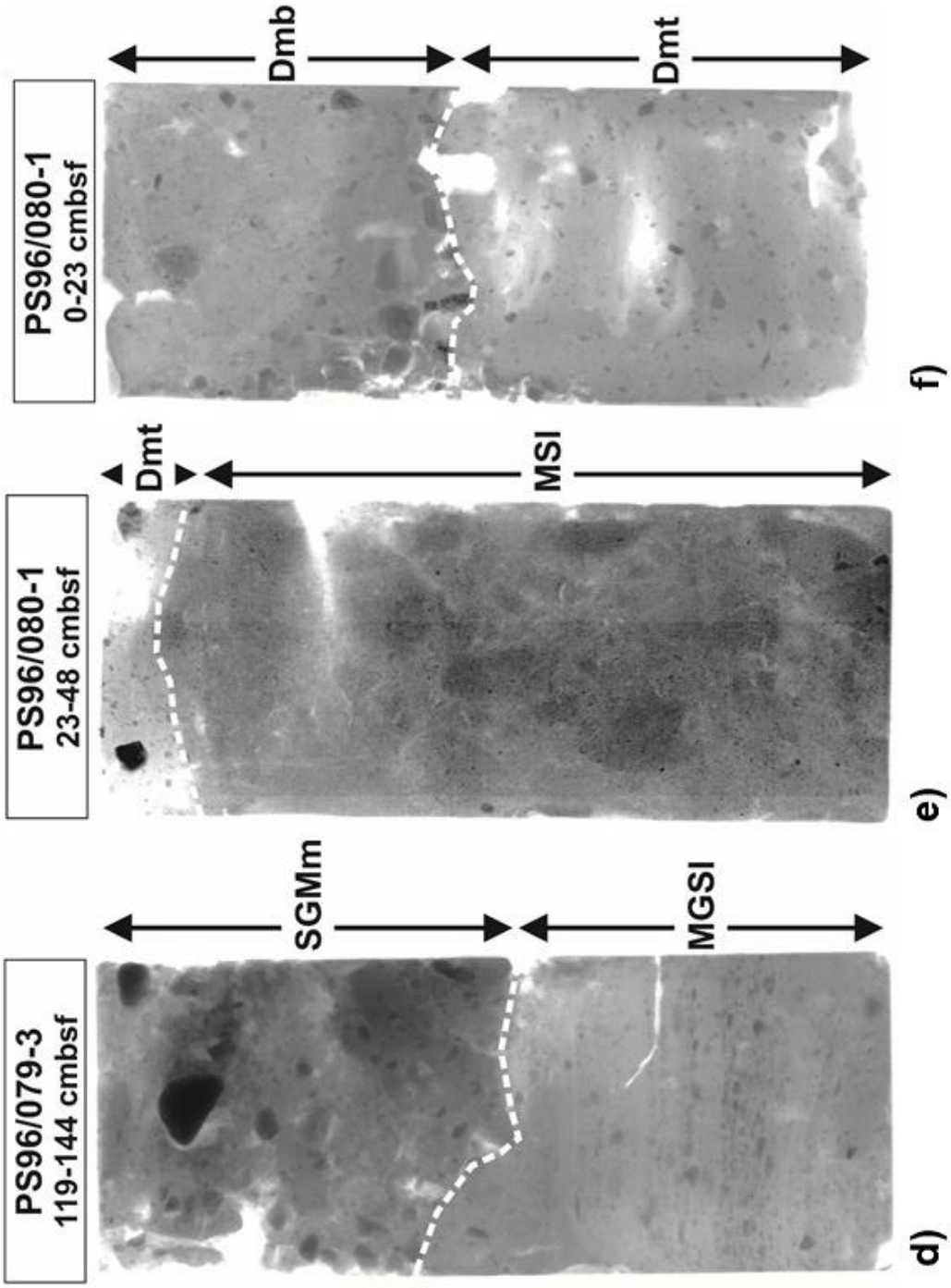

111

112

Figure DR5 (continued)

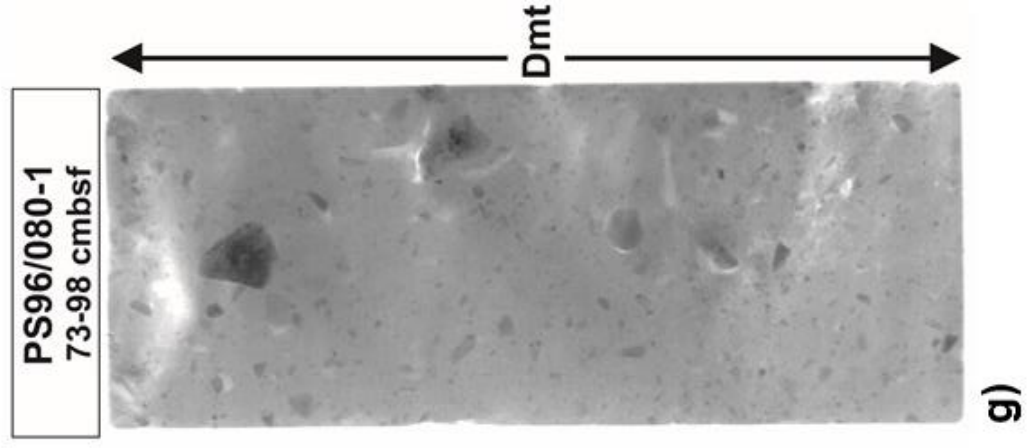

Figure DR6 (next page): Sample horizons of AMS ^{14}C dated foraminifer shells in cores PS96/079-3 and PS96/080-1 (orange boxes) in relation to sediment lithology visualised by X-radiograph positives. a) PS96/079-3 17 cmbsf (cm below surface): b) PS96/079-3 150 cmbsf: c) PS96/080-1 20 cmbsf; d) PS96/080-1 120 cm cmbsf. Each X-radiograph is 10 cm wide, and white areas are voids in the sediment slabs caused by large gravel grains/pebbles or sample processing. For details of AMS ^{14}C dates, see Table DR2.

PS96/079-3
0-25 cmbsf
a)
PS96/079-3
144-169 cmbsf
b)
PS96/080-1
0-23 cmbsf
c)
PS96/080-1
98-123 cmbsf
d)

127

128

SUPPLEMENTARY REFERENCES

Anderson, J. B., and Andrews, J. T., 1999, Radiocarbon constraints on ice sheet advance and retreat in the Weddell Sea, Antarctica: Geology, v. 27, p. 179-182.

Arndt, J. E., Schenke, H. W., Jakobsson, M., Nitsche, F. O., Buys, G., Goleby, B., Rebesco, M., Bohoyo, F., Hong, J.-K., Black, J., Greku, R., Udintsev, G., Barrios, F., Reynoso-Peralta, W., Taisei, M., and Wigley, R., 2013, The International Bathymetric Chart of the Southern Ocean (IBCSO) Version 1.0 - A new bathymetric compilation covering circum-Antarctic waters: Geophysical Research Letters, v. 40, p. 3111-3117.

Domack, E.W., Jacobson, E.A., Shipp, S., and Anderson, J.B., 1999, Late Pleistocene-Holocene retreat of the west Antarctic ice-sheet system in the Ross sea: Part 2. Sedimentologic and stratigraphic signature: Geological Society of America Bulletin, v. 111, p. 1517-1536.

Heroy, D.C., and Anderson, J.B., 2007, Radiocarbon constraints on Antarctic Peninsula Ice Sheet retreat following the Last Glacial Maximum (LGM): Quaternary Science Reviews, v. 26, p. 3286-3297.

Hillenbrand, C.-D., Larter, R.D., Dowdeswell, J.A., Ehrmann, W., Ó Cofaigh, C., Benetti, S., Graham, A.G.C., and Grobe, H., 2010, The sedimentary legacy of a palaeo-ice stream on the shelf of the southern Bellingshausen Sea: clues to West Antarctic glacial history during the Late Quaternary: Quaternary Science Reviews, v. 29, p. 2741-2763.

Hillenbrand, C.-D., Melles, M., Kuhn, G., and Larter, R. D., 2012, Marine geological constraints for the grounding-line position of the Antarctic Ice Sheet on the southern Weddell Sea shelf at the Last Glacial Maximum: Quaternary Science Reviews, v. 32, p. 25-47.

McKay, R., Browne, G., Carter, L., Cowan, E., Dunbar, G., Krissek, L., Naish, T., Powell, R., Reed, J., Talarico, F., and Wilch, T., 2009, The stratigraphic signature of the late Cenozoic Antarctic Ice Sheets in the Ross Embayment: Geological Society of America Bulletin, v. 121, p. 1537-1561.

McKay, R., Naish, T., Powell, R., Barrett, P., Scherer, R., Talarico, F., Kyle, P., Monien, D., Kuhn. G., Jackolski, C., and Williams, T., 2012, Pleistocene variability of Antarctic Ice Sheet extent in the Ross Embayment: Quaternary Science Reviews, v. 34, p. 93-112.

Miller, H., and Oerter, H. (eds.), 1991, The Expedition ANTARKTIS-VIII of RV "Polarstern" 1989/1990 – Report of Leg ANT-VIII/5: Reports on Polar and Marine Research, v. 86, 155 pp.

Passchier, S., Browne, G., Field, B., Fielding, C.R, Krissek, L.R, Panter, K., Pekar, S.F., and the ANDRILL-SMS Science Team, 2011, Early and middle Miocene Antarctic glacial history from the sedimentary facies distribution in the AND-2A drill hole, Ross Sea, Antarctica: Geological Society of America Bulletin, v. 123, p. 2352-2365.

RAISED Consortium, 2014, A community-based geological reconstruction of Antarctic Ice Sheet deglaciation since the Last Glacial Maximum: Quaternary Science Reviews, v. 100, p. 1-9.

Reimer, P. J., Bard, E., Bayliss, A., Beck, J. W., Blackwell, P. G., Bronk Ramsey, C., Buck, C. E., Cheng, H., Edwards, R. L., Friedrich, M., Grootes, P. M., Guilderson, T. P., Haflidason, H., Hajdas, I., Hatté, C., Heaton, T. J., Hoffmann, D. L., Hogg, A. G., Hughen, K. A., Kaiser, K. F., Kromer, B., Manning, S. W., Niu, M., Reimer, R. W., Richards, D. A., Scott, E. M., Southon, J. R., Staff, R. A., Turney, C. S. M., and van der Plicht, J., 2013, INTCAL13 and MARINE13 radiocarbon age calibration curves, 0–50,000 years cal BP: Radiocarbon, v. 55, no. 4, p. 1869-1887.

Schröder, M. (ed.), 2016, The Expedition PS96 of the Research Vessel POLARSTERN to the southern Weddell Sea in 2015/2016: Reports on Polar and Marine research, v. 700, 143 pp.

Stolldorf, T., Schenke, H.-W., and Anderson, J. B., 2012, LGM ice sheet extent in the Weddell Sea: evidence for diachronous behavior of Antarctic Ice Sheets: Quaternary Science Reviews, v. 48, p. 20-31.

Stuiver, M., and Reimer, P.J., 1993, Extended ^{14}C data base and revised CALIB 3.0 ^{14}C age calibration program: Radiocarbon, v. 35, p. 215-230.

Tripsanas, E., Piper, D.J.W., Jenner, K.A., and Bryant, W.R., 2008, Submarine mass-transport facies: new perspectives on flow processes from cores on the eastern North American margin: Sedimentology, v. 55, p. 97-136.

Wacker, L., Bonani, G., Friedrich, M., Hajdas, I., Kromer, B., Němec, M., Ruff, M., Suter, M., Synal, H. A., and Vockenhuber, C., 2010, MICADAS: Routine and High-Precision Radiocarbon Dating: Radiocarbon, v. 52, no. 2-3, p. 252-262.